



Objective climatology and classification of the Mediterranean cyclones based on the ERA5 data set and the use of the results for the definition of seasons

G. Kotsias¹ · C. J. Lolis¹ · N. Hatzianastassiou¹ · N. Bakas¹ · P. Lionello² · A. Bartzokas¹

Received: 7 September 2022 / Accepted: 14 January 2023 / Published online: 26 January 2023
© The Author(s) 2023

Abstract

An objective cyclone detection and tracking analysis is performed for the Mediterranean region with the use of 6-hourly (00, 06, 12, and 18 UTC) $1^\circ \times 1^\circ$ mean sea-level pressure data obtained from the ERA5 database for the period 1950–2018. At first, the main cyclogenesis and high-density areas of cyclones are identified. Next, principal component analysis and cluster analysis are performed, classifying the detected cyclone trajectories into 12 clusters. In the following step, the application of the above methodology, this time on the intra-annual variations of the 12 cyclone clusters' frequencies leads to the objective definition of four seasons, which generally correspond to the conventional ones, but they present differences in their limits and duration. The results of this method are also compared with the ones of two other methods for defining the seasons, which are based (i) on the long-term mean intra-annual variations of various meteorological parameters and (ii) on the intra-annual variations of the frequencies of defined weather types, revealing larger winter and shorter spring seasons. Finally, a composition of all three aforementioned approaches is attempted, leading to the following seasons: “winter” (November 16–March 25) which lasts more than 4 months, “spring” (March 26–June 11) with a duration of approximately 2.5 months, “summer” (June 12–September 12) which lasts about 3 months, and “autumn” (September 13–November 15) with a duration of about 2 months. The long-term changes of the above seasons' characteristics are also examined.

1 Introduction

The study of cyclones and their characteristics has always been one of the most important and challenging subjects of atmospheric sciences. The Mediterranean basin is a geomorphologically complex region that combines multiple climate types and is a well-known area of frequent cyclone formation (Trigo et al. 1999; Maheras et al. 2001; Lionello et al. 2002, 2006; Alpert et al. 2004a; Trigo 2006). Cyclones play a key role in synoptic-scale variability and are connected to extreme weather events resulting in huge property damages as well as human casualties. Therefore, the study of cyclones and their characteristics is a vital subject involving the agricultural, socioeconomic, tourism, and health regimes

of the Mediterranean. A recently published article by Flaounas et al. (2022) summarizes the current knowledge about the Mediterranean cyclones, including the various subtypes, their climatology, their relationship with large-scale atmospheric circulation, their dynamics, and their impacts on weather, while also provides insight for their prediction and future trends.

There are many algorithms and methodologies which have been used in previous studies for the examination of cyclones, including the identification of cyclone centers and the associated tracks. The meteorological parameters used in such a process can also vary. The parameter used in most studies dealing with cyclone detection and tracking is the mean sea-level pressure (MSLP) (Murray and Simmonds 1991; Simmonds and Murray 1999; Lionello et al. 2002; Pinto et al. 2005; Trigo 2006; Wernli and Schierz 2006; Akperov et al. 2007; Wang et al. 2006; Reale and Lionello 2013). Other variables used in previous studies include the geopotential height at 1000 hPa (Blender et al. 1997; Raible et al. 2008) and the vorticity at 850 hPa (Sinclair 1997; Inatsu 2009; Flaounas et al. 2014). Blender et al. (1997) developed a cyclone detection and tracking algorithm in order to identify the cyclone track regimes

✉ G. Kotsias
g.kotsias@uoi.gr

¹ Laboratory of Meteorology, Department of Physics, University of Ioannina, 45110 Ioannina, Greece

² Department of Biological and Environmental Sciences and Technologies, University of Salento, Lecce, Italy

over the North Atlantic by using 6-hourly data of geopotential height at 1000 hPa (z1000) from the ECMWF database with a spatial resolution of $1.1^\circ \times 1.1^\circ$, for the 1990–1994 winters. According to their algorithm, a cyclone is defined as a local minimum in the z1000 field in a 3×3 grid point field, and the trajectories of the cyclones are determined by using the nearest-neighbor method in the preceding z1000 field. Trigo et al. (1999) also applied Blender's algorithm but for the Mediterranean region and for a longer time period. Pinto et al. (2005) used 6-hourly MSLP data from NCEP/NCAR and applied their cyclone detection and tracking algorithm for the Northern Hemisphere and for two winters. According to their algorithm, a SLP minimum is considered as a cyclone center if it is at least 4 hPa below the mean pressure of 20 surrounding grid points, and a minimum value of pressure gradient in the 3×3 area surrounding is required. For the cyclone tracking, for each identified cyclone, the algorithm predicts a subsequent position by using a "prediction velocity", and from the identified cyclones in the preceding field, the most likely candidate is chosen. Trigo (2006) applied a cyclone detection and tracking algorithm for the Euro-Atlantic sector by utilizing 6-hourly z1000 data from NCEP/NCAR ($2.5^\circ \times 2.5^\circ$) and ERA-40 ($1.125^\circ \times 1.125^\circ$), for the extended winter period of 1958–2000. According to that cyclone detection algorithm, a z1000 local minimum is considered a possible cyclone center if the minimum is not higher than 165 gpm, and the geopotential gradient, averaged over an area of about 1000^2 km^2 , is at least 4.5 gpm/100 km. These thresholds were adjusted empirically for the Mediterranean. The cyclone tracking is based on a nearest-neighbor search in the previous field. Bartholy et al. (2009) used 6-h MSLP data from ERA-40 ($1^\circ \times 1^\circ$) to study the genesis and intensity of cyclones in the Atlantic-European region and the western Mediterranean. In the cyclone detection part of the algorithm, the potential cyclone centers must have SLP less than 1000 hPa in the N Atlantic-Europe region (1013.5 hPa for western Mediterranean), and they must be centers of pressure minima in a 5×5 grid box. Cyclone tracks are determined by special sequences of stored potential cyclone centers. Flaounas et al. (2014) worked on tracking winter extra-tropical cyclones by using 6-hourly data of relative vorticity at 850 hPa from ERA-Interim ($1.5^\circ \times 1.5^\circ$) for the winters of the period 1989–2009. The cyclone detection algorithm they used carried out the procedure in three steps. First, the algorithm identifies all cyclonic circulations, and a spatial smoothing of the vorticity field is applied. Then, for each cyclonic circulation, the algorithm identifies all of its representative centers which are treated as different cyclones. Finally, for each center, the algorithm quantifies its characteristics. In the cyclone tracking part of the algorithm, all the identified cyclones are sorted based on their relative vorticity, from the strongest to the weakest, and then, the algorithm starts from the first cyclone and searches forward and backward in time for all its undergoing possible tracks and the track

for which the feature presents the most "natural evolution" of relative vorticity is chosen. In the present work, the algorithm used for the cyclone detection and tracking process has been introduced and analyzed in detail in the paper of Lionello et al. (2002). In the "Methodology" section, a brief description of the algorithm is presented.

Obviously, the choice of the tracking method affects the tracks (their origins, paths, and lengths) and the characteristics of the cyclones. Consensus and disagreement among different tracking methods have been investigated in the IMILAST project (Intercomparison of Mid-Latitude STorm diagnostics) at global (Neu et al. 2013) and Mediterranean regional scale (Lionello et al. 2016). In general, differences among methods are large concerning the overall number of cyclones and the tracks of weak cyclones, while there is a substantial agreement on inter-annual variability of cyclone numbers, on the most pronounced geographical patterns and on the life cycle characteristics. In the Mediterranean, there is an agreement on the main cyclogenesis areas (in the northwestern and Levantine basins and North Africa), the variability, the sign, and the significance of ongoing trends.

After the study and analysis of the cyclones affecting the Mediterranean region, an objective method for the climatological definition of seasons is attempted, by utilizing the intra-annual variations of the cyclones' frequencies. Such a method of seasons' definition has never been attempted/presented in previous studies, and thus, the present work provides a "new" and important addition to the community of climate research. This procedure is based on the objective classification of cyclone tracks performed with the use of a classification technique including principal component analysis and *k*-means cluster analysis. Moreover, this method of seasons' definition (cyclone tracks' frequency (CTF) method) is compared with two other seasons' definition methods: the meteorological variables' mean intra-annual variation (MVV) method introduced in Kotsias et al. (2020b) and the weather types' frequency (WTF) method applied in Kotsias et al. (2021). Finally, a composite (C) method which combines the CTF, MVV, and WTF methods is followed. Changes in the seasons' characteristics (limits and duration) are also investigated. This total research work provides a complete attempt on the definition of seasons by taking into account multiple variables and methodologies, while the differences between the methods will indicate the sensitivity of the approach followed for the objective delimitation of seasons.

2 Data and methodology

2.1 Data

In the present work, the mean sea-level pressure (MSLP) is used for the cyclone detection and tracking. The data

Fig. 1 The geographical domain of the analysis. The outer border defines the domain used for the detection of the cyclone centers and the inner border defines the domain used for the classification of the tracks and the definition of seasons

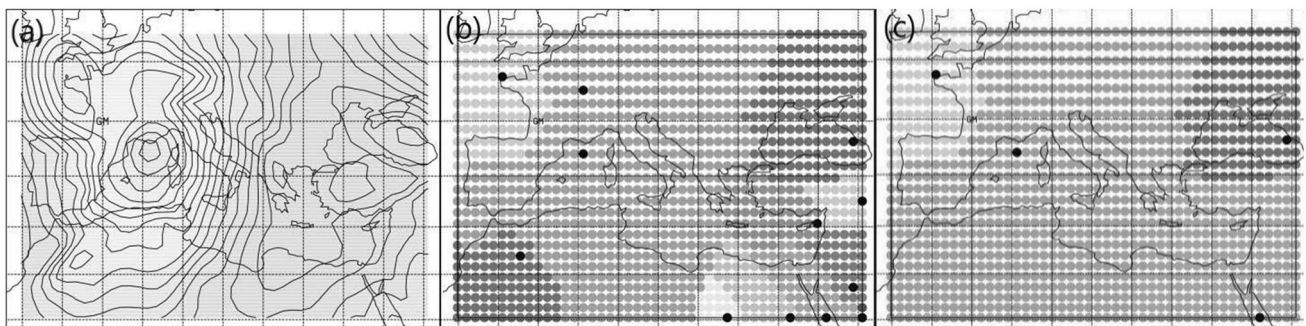
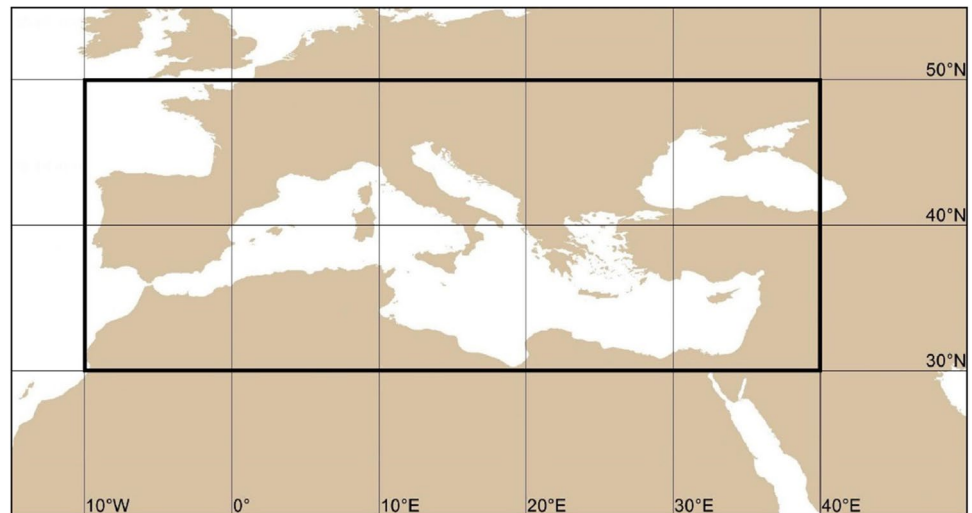


Fig. 2 Example of the procedure for the identification of the cyclones. **a** Original sea-level pressure (SLP) field. **b** Results of the partitioning procedure. Each dot represents a grid point, and the dots with the same gray level belong to the same partition. Black dots show the location of the pressure minimum of each partition. **c** Final

set of large depressions that result from the merging of the small depressions whose central minimum is at a distance less than 4 grid points from the boundary of a different and deeper depression. From Lionello et al. (2002)

are obtained from the European Centre for Medium-Range Weather Forecasts (ECMWF) ERA5 reanalysis (Copernicus Climate Change Service 2017; Hersbach et al. 2020), which is the most recent state-of-the-art database providing high spatial–temporal resolution and high-quality data. The data used have a spatial resolution of $1^\circ \times 1^\circ$ and a temporal resolution of 6 h from 1/1/1950 to 31/12/2018. This choice is consistent with previous studies (Neu et al. 2013; Lionello et al. 2016), in which the tracking method used was shown to reproduce efficiently all of the most representative features of the Mediterranean region. Investigating the advantages of high resolution to properly detect small-scale cyclones and fine structures is outside the scope of this study. Further, note that the tracking method adopted in this study ignores shallow features close to large cyclonic circulations, and this limits the dependence of the results from the resolution of the input fields. The data consider the geographical domain shown in Fig. 1 (55°N – 20°N and 15°W – 50°E), which includes

the central and southern Europe, northern Africa, and SW Asia.

2.2 Methodology

In this work, the cyclone detection and tracking algorithm introduced in the work of Lionello et al. (2002) are used (an example is shown in Fig. 2). The algorithm uses 6-hourly sea-level pressure (SLP) data. At first, the procedure partitions the SLP fields (Fig. 2a) in sets of different depressions. For each grid point, a “steepest descent path” connecting it to the nearest-neighbor grid point with the lowest SLP value is identified and continued until a local minimum, where the SLP value is lower than the SLP at the 8 nearest grid points reached (Fig. 2b). A depression is made of all points crossed by a path leading to the same minimum. Small depressions whose central minimum is at a distance less than 4 grid points from the boundary of a different and deeper depression are included in the latter. This criterion has led to the

exclusion of the minimum south of the Atlas Mountain in Fig. 2b from the set of large depression systems, in which the whole map is partitioned at the end of the first part of the tracking procedure (Fig. 2c). Note that this minimum could be tracked as an independent cyclone in its following evolution, if, in the following time steps, it would become sufficiently deep and well-separated from the rest of the circulation.¹ Each of the systems in Fig. 2c is characterized with a center, which is slightly shifted with respect to the location of the pressure minimum to account for its asymmetric spatial distribution, and with a “radius” R , which is computed as the average distance of the grid points in the low-pressure system from its center. The second part of the procedure identifies the cyclone tracks by joining the location of low-pressure centers with minimum displacement in successive maps. The search for the candidate center is limited by a maximum allowed displacement, which increases with radius R of the cyclone, its former speed, and is longer in the zonal than in the meridional direction to account for eastward mean motion of cyclones in the Mediterranean region. When no center is found, cyclone termination is assumed. The process, therefore, includes a track, an initial and a final position of a cyclone, a sequence of pressure minima, and a sequence of areas covered by the cyclone. This algorithm was also applied in the work of Reale and Lionello (2013), and more details can be found in the paper of Lionello et al. (2002).

The aforementioned cyclone detection and tracking algorithm is applied to the outer domain shown in Fig. 1. The minimum duration of the accepted cyclone tracks is 18 h, and as such, the majority of the detected cyclones is included in the analysis independently of their characteristics (e.g., dynamical or thermal). Only the cyclones entering the inner domain, i.e., the Mediterranean region (50°N – 30°N and 10°W – 40°E , Fig. 1) at least once in their lifetime, are kept for the analysis. The inner domain is adopted for consistency with the definitions of the seasons in previous studies (Kotsias et al. 2020b, 2021). The outer domain is required to avoid problems with spurious tracks and cyclogenesis along the boundaries of the area of interest.

In the next step, various tests are performed to find the best possible methodology to proceed to the classification of the cyclone tracks as needed for the seasons’ definition. The classification method adopted in this work requires that all cyclone tracks have the same length in terms of number of grid points. Taking this under consideration, multiple methods have been tested for processing the cyclone tracks

and reducing them to the same number of points, including the interpolation method, the calculation of the distances among the tracks, and the calculation of the discrete Fréchet distances (Champers et al. 2009). The method leading to the most realistic and physically interpretable results was found to be the linear interpolation of the coordinates of the cyclone tracks to a predefined number of geographical points, which is equal to the life of the longest-lived cyclone detected (in number of 6-h intervals).

Two statistical methods are used in this work: principal component analysis (PCA) and cluster analysis (CA).

PCA is a dimensionality reduction technique commonly used in climatological studies when a very large amount of data is encountered. The aim of PCA is to reduce the number of variables of a data set, while preserving as much information as possible. It is a multivariate statistical method that extracts a small number of new uncorrelated variables (PC1 , PC2 , ..., PCm), called principal components (PCs), which are constructed as linear combinations of the initial variables, while most of the initial variance is accounted for by the first components. Also, varimax rotation of the axes is applied, in order to maximize the discrimination among the initial variables (Jolliffe 1986; Richman 1986). CA is a statistical method that classifies the cases of a set of variables into objectively defined and distinct groups, called clusters. In the present work, k -means CA is applied (Sharma 1995; Kalkstein et al. 1996). In the k -means method, the algorithm establishes the presence of clusters by finding their centroid points, where a centroid point is the average of all the data points in the cluster. By assessing the Euclidean distance between each point in the data set, each one can be assigned to a cluster. The optimum number of clusters is indicated by the distortion test (Sugar and James 2003).

The complete steps of the methodology followed in this work are shown in Fig. 3. After the run of the cyclone detection and tracking algorithm, the application of the criterion to exclude the cyclones that do not cross the Mediterranean, and the interpolation of the cyclones’ coordinates, a matrix is constructed. The rows of this matrix are equal to the number of cyclones (22,404), and the columns refer to the two geographical coordinates ($2 \times 268 = 536$). It is noted that 268 (in 6-h intervals, equal to 67 days) is the lifetime of the longest-lived cyclone detected. Then, “spectral analysis” is applied, which involves the application of a dimensionality reduction technique (PCA) followed by a classification procedure (CA), and groups/clusters of cyclone tracks are formed based on their spatial characteristics. Next, the date-to-date intra-annual variations of the frequencies of the defined cyclone clusters are calculated. These values are replaced by the 5-day moving averages in order to achieve the necessary smoothing and noise reduction. Finally, “spectral analysis” is applied again, now on the time-series of the intra-annual variations of the cyclone clusters’ frequencies,

¹ Note that this tracking method does reproduce the well-known cyclogenesis south of the Atlas, as it is shown in the original paper (Lionello et al. 2002), in other maps produced by it (e.g., Fig. I.16 of Lionello et al. 2012) and by the results of this study.

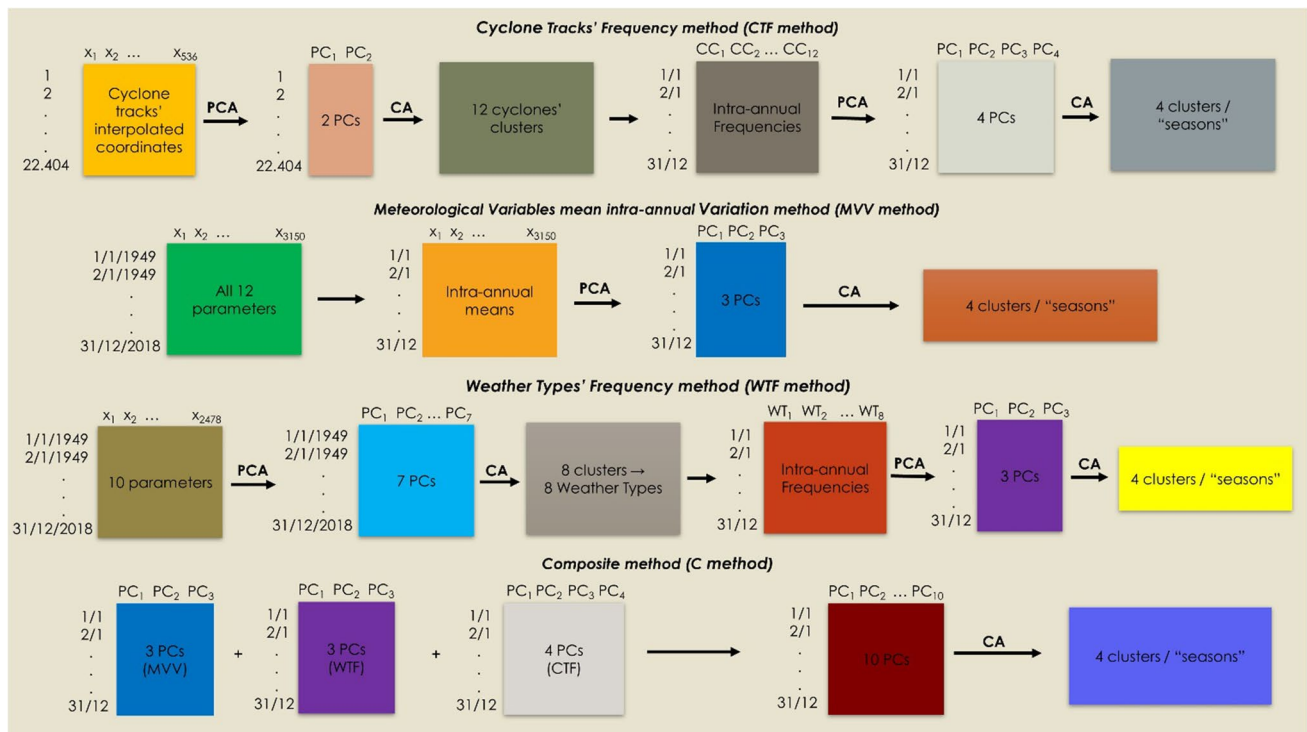


Fig. 3 Schematic representation of the four methods applied for the definition of seasons: the CTF, WTF, MVV, and C methods

grouping dates within the year with similar frequency distribution among the cyclone clusters and thus resulting in the definition of seasons. This method of seasons' definition is called cyclone tracks' frequency (CTF) method.

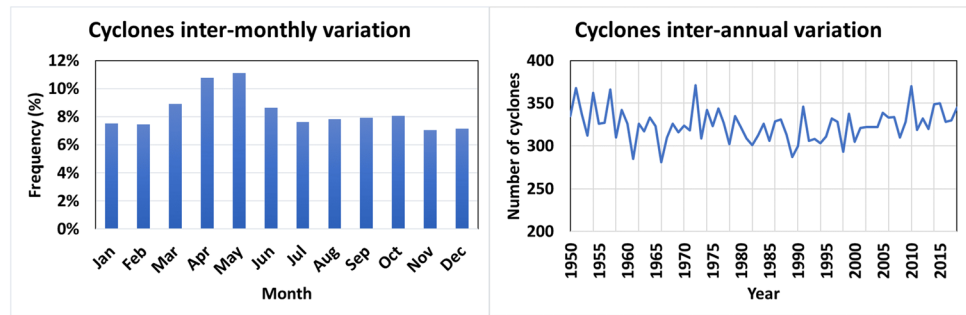
Furthermore, the CTF method is compared and combined with two other methods for the definition of seasons: the meteorological variables' mean intra-annual variation (MVV) method introduced in Kotsias et al. (2020b) and the weather types' frequency (WTF) method followed by Kotsias et al. (2021).

These two methods, MVV and WTF, used daily (12UTC) grid point data for the Mediterranean region (50°N–30°N and 10°W–40°E, Fig. 1 inner box) and for the 70-year period 1949–2018. The data were obtained from the NCEP/NCAR and consist of the following 12 meteorological parameters: air temperature and zonal and meridional wind components at 2 m above ground level, precipitation and convective precipitation, total cloud cover, geopotential height at 500 hPa and 1000 hPa, air temperature at 500 hPa and 850 hPa, specific humidity at 850 hPa, and precipitable water. It is worth noting that compared to the data used in the MVV method, the parameters of precipitation and convective precipitation were not included in the WTF method due to the high percentage of daily zero values, which made their introduction into the statistical analysis problematic. Instead, total cloud cover, which is significantly associated with precipitation, was used (Bartzokas and Metaxas 1995).

In the MVV method (Kotsias et al. 2020b), the mean intra-annual variations of the 12 meteorological parameters are calculated and entered in a matrix (365 days of the year \times 3150 grid points multiplied by the number of parameters). These mean values are replaced by the 5-day moving averages to achieve the necessary smoothing. PCA is then applied, and then, CA is performed resulting in the classification of the dates within the year into clusters. Each cluster contains the dates of the year with homogeneous climatic characteristics related to the magnitude and the patterns of specific climatic parameters in the Mediterranean region and therefore constitutes the objectively defined seasons.

In the WTF method (Kotsias et al. 2021), a matrix is created that contains the daily values (1/1/1949–31/12/2018) of the 10 meteorological parameters. Then, PCA and CA are applied resulting in the classification of the dates into clusters. Each cluster contains dates that show similar weather/synoptic conditions and therefore defines a weather type (WT). Eight WTs are defined. Next, a matrix containing the 5-day moving averages of the mean date-to-date intra-annual variations of the frequencies of the defined WTs is constructed. The rows in this matrix correspond to the days of the year (365), and the columns refer to the daily frequencies of the 8 specified WTs. PCA and CA are applied again, this time on the matrix of the intra-annual variations of the WTs' frequencies, classifying the dates within the year that

Fig. 4 The inter-monthly (%) and inter-annual variations of the frequency of the cyclones affecting the Mediterranean region



show a similar distribution of WTs' frequencies into clusters and thus objectively defining the seasons.

Finally, a fourth method (method C) is introduced in the present work in order to define the seasons, which is essentially the composition of the other three methods, i.e., the CTF, the MVV, and the WTF methods. The C method is performed by applying CA to the unified matrix of the PCs of the three individual methods. The selection of the domain (Fig. 1) and time period (1950–2018) for the application of the cyclone detection and tracking procedure was done in order for a common ground to exist in the comparison of the CTF method presented in this work with the two methods, MVV and WTF, from the previous studies. The steps of all four methods (CFT, MVV, WTF, and C) are shown in detail in Fig. 3, where a schematic representation of all the applied methodologies is shown.

In each of the three methods (CTF, WTF, and MVV), as well as in their composition (C), the whole process followed for the total 70-year period 1949–2018 was also carried out for the five overlapping 30-year subperiods 1949–1978, 1959–1988, 1969–1998, 1979–2008, and 1989–2018, in order to examine the long-term changes of the main characteristics of the defined seasons (limits and duration).

3 Results and discussion

3.1 Cyclone tracks clustering

The application of the cyclone detection and tracking algorithm for the outer domain shown in Fig. 1 leads to the detection of 40.472 cyclones. After, the application of the criterion to exclude cyclones which never enter the inner domain of the Mediterranean region, 22.404 cyclones remain. The inter-monthly (%) and inter-annual (in number of cyclones) variations of the frequency of the detected cyclones are shown in Fig. 4. On average, 325 cyclones are detected each year, and there seems to be a higher cyclone activity during spring. The high frequency of cyclones in April and May can be attributed to the fact that during these months, significant cyclone activity appears over the land due to the intense land warming and the upper air disturbances, while

cyclonic activity over the sea still exists also (ending later in conventional summer). Also, the possible existence of statistically significant (95% confidence level) linear trends has been investigated using the Mann–Kendall test (Kendall 1975), and no such trend was found. It should be noted that in the calculation of the inter-monthly frequencies, each cyclone is counted multiple times since it is present during more than one consecutive 6-h interval. Figure 5 shows the spatial distributions of track density and cyclogenesis. In general, the high cyclogenesis areas coincide with those of high density. The area with the highest cyclonic activity, where most cyclones pass or are formed, is the Gulf of Genoa in the northwest Mediterranean and follows the paths along the Adriatic, the Tyrrhenian, and the Ionian Seas. Another high cyclogenesis/density area is seen south of the Atlas Mountain range where the cyclones are formed and move towards the central part of the basin. Also, the area of the formation of Cyprus lows is evident in SE Mediterranean. Other large activity areas include the Black Sea, the Aegean Sea, and the Middle East. These findings are in very good agreement with the results of Lionello et al. (2016) where multiple cyclones detecting and tracking algorithms and their results are compared.

In the next step, a matrix is constructed where the rows correspond to the cyclones (22.404) and the columns to the 268 pairs of linearly interpolated coordinates ($2 \times 268 = 536$ columns) and a spectral analysis procedure are performed on that matrix, i.e., the application of PCA followed by the application of CA. The application of PCA on the matrix of the interpolated coordinates of the cyclones led to 2 PCs which explain 93% of the total variance. The application of CA on the series of the 2 PCs led to 12 clusters of cyclone tracks. The selection of the number of clusters was decided by taking into account the distortion test (Sugar and James 2003) as well as considering the best possible classification of the cyclone tracks leading to physical interpretable results. In fact, the distortion test indicated that the optimum number of clusters could be either 7, 12, or 16. The classification procedure was carried out for each of the above number of clusters, and it was finally concluded that the choice of 12 clusters leads to the best possible classification, characterized by the spatially most homogeneous and discrete

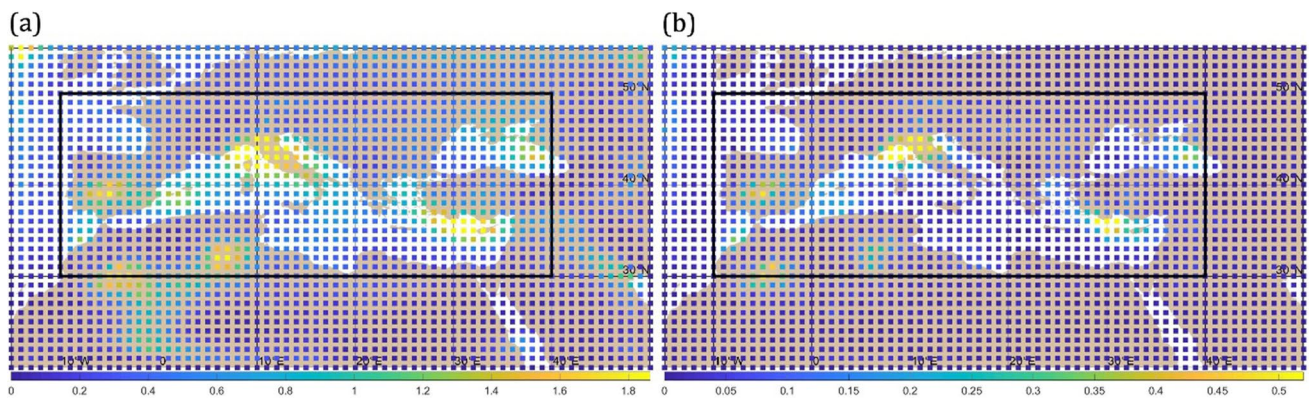


Fig. 5 Cyclone tracks and cyclogenesis in the Mediterranean region. **a** Track density. The colors represent the probability (%) that a cyclone track crosses every 1×1 cell in the area over a period of 6 h.

b Probability (%) of cyclogenesis occurring in each cell within the 6-h field. In both panels, only the cyclones whose path crosses the Mediterranean region (large rectangle) are taken into account

groups. Each cluster represents a group of cyclones with similar tracks. The spatial distributions of the 12 cyclone tracks clusters (hereafter CCs) are shown in Fig. 6. Each black curve corresponds to a track. The red curve corresponds to the track with the shortest distance from the corresponding cluster center, while the green curve is the mean track of the corresponding cluster, which is calculated as the average value of the coordinates (longitude and latitude) of all the tracks belonging to the cluster. Figure 7 shows the inter-monthly variations of the frequencies of the 12 CCs, and Table 1 shows the characteristics of the CCs, including their names, seasonality, average central MSLP, and the number of cyclones classified in each cluster as well as their mean annual frequency.

The first CC (CC1, central Europe) contains 1546 cyclone tracks that occur throughout the year with a higher frequency of occurrence during the warm period of the year (April–August). In general, these cyclones are formed in western or central Europe north of the Mediterranean Sea and move towards eastern Europe. Such cyclones are more frequent during the warm period of the year, because of the contribution of the diabatic heating associated with the intense solar radiation to the cyclonic activity over continental regions (Metaxas 1978). These cyclones are mainly connected to the passage of organized upper-level troughs from NW Europe towards central Europe which triggers the formation of surface cyclones, with frontal activities or not (Campins et al. 2011).

CC2 (Cyprus lows) includes a relatively small number of cyclone tracks (833) which occur mainly during spring and autumn. The cyclones of this cluster are mainly formed in the eastern Mediterranean west of Cyprus and move eastwards along the Mediterranean Sea axis, affecting the weather conditions of the neighboring areas including southern Turkey and the Middle East. It must be noted that the majority of the cyclones in the SE Mediterranean

area propagating towards the Cyprus region do not present the typical frontal structure (Shapiro and Keyser 1990) and are mainly accompanied by occluded fronts or vortex characteristics (absence of fronts).

CC3 (North Med – cold season) consists of 1617 cyclone tracks which are frequent mainly during the cold period of the year (November–March). This cluster contains the cyclones that are formed over the main cyclogenesis regions of the central and northern Mediterranean Sea and move towards the eastern Mediterranean affecting the weather conditions of the surrounding areas (Trigo et al. 1999; Maheras et al. 2001), including Italy, Greece, and Turkey. Such cyclones are mainly the frontal depressions formed during the cold period of the year because of the high baroclinicity along the northern Mediterranean coasts and the high sensible heat over the warm (relatively to the overlying air) sea surface, contributing to significant precipitation amounts over the above regions (Trigo et al. 2002; Reale and Lionello 2013; Kotsias et al. 2020a).

CC4 (Sharav cyclones – Africa) includes 1684 cyclones that occur throughout the year with a frequency peak in spring. These depressions, known as Sharav cyclones or Saharan depressions, are a dominant feature of the Mediterranean spring, as the area south of the Atlas Mountain range becomes a major source of cyclogenesis which peaks in May–June. Cyclogenesis, not only on the lee of the Atlas Mountains, but also in all the southern parts of western and central Mediterranean (including the northern African coasts), is primarily regulated by the conceptual model of “finite amplitude” cyclogenesis (Hoskins et al. 1985), which is also analyzed in Thorncroft and Flocas (1997). In simple words, the result of the potential vorticity conservation in adiabatic motions, when organized upper-level troughs propagate towards the Mediterranean area from northern latitudes and interact with a pre-existed low-level baroclinic zone over the southern Mediterranean

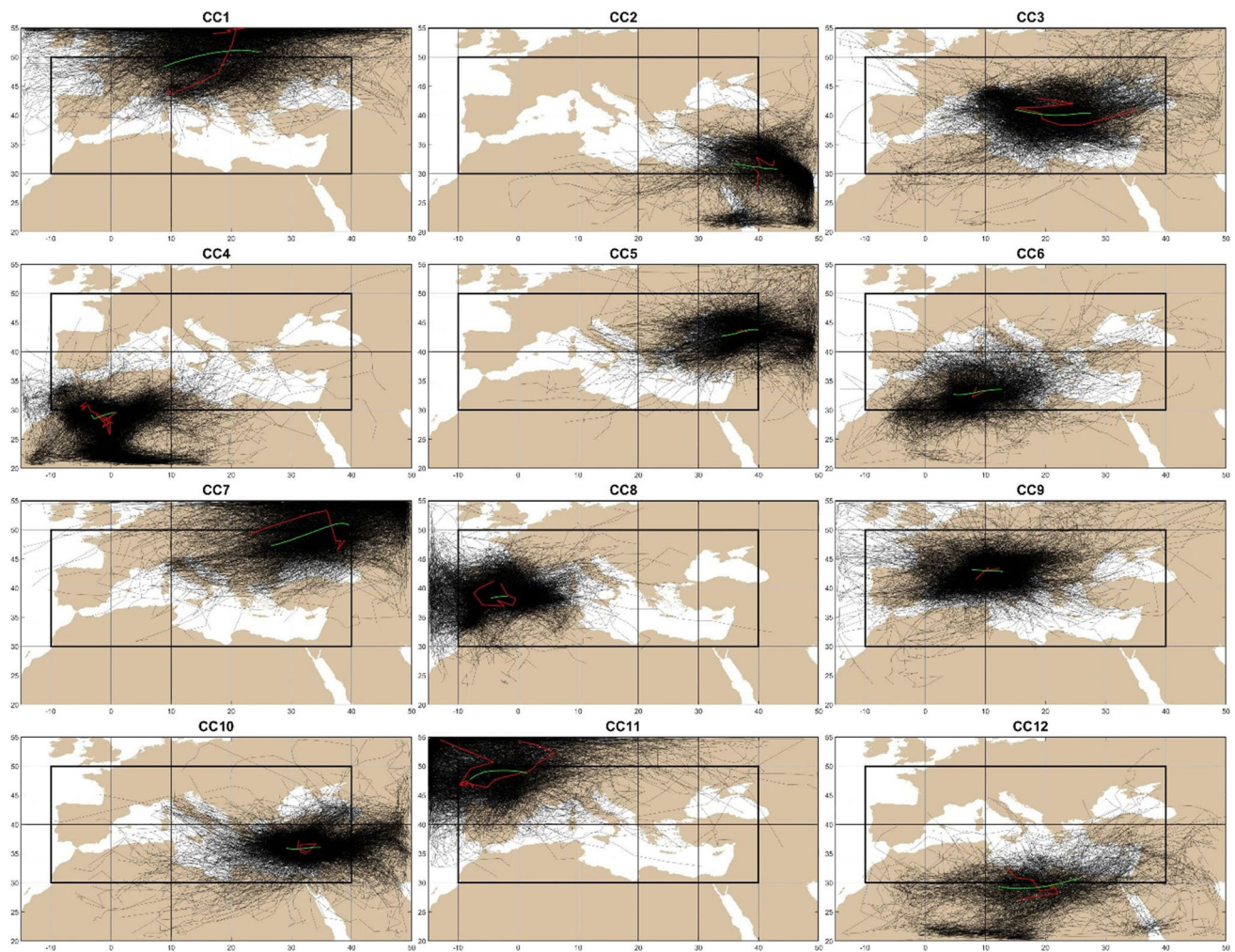


Fig. 6 The cyclone tracks of the 12 clusters. The red curves correspond to the cyclone tracks with the shortest distance from the corresponding cluster center. The green curves are the mean tracks of the corresponding clusters

parts, plays a crucial role, among all the other factors (like orography).

CC5 (Black Sea) consists of 1861 cyclones, which show similar frequency distribution during all months. They are cyclones that are formed in the region of the Black Sea and affect the areas of the northeastern Mediterranean region, as well as regions of SE Europe and W Asia. The Black Sea region has been shown to be one of the main cyclogenesis centers of the greater eastern Mediterranean region, being active throughout the year (Trigo et al. 1999).

CC6 (Sharav cyclones – central Med) comprises of 1,605 depressions that occur throughout the year with a frequency maximum in spring. Such depressions, formed over the regions of NW Africa, specifically west of Tunisia, can also be considered as Sharav cyclones that are characterized by a more eastward movement compared to the ones of CC4. They are intensified passing over the Mediterranean Sea east of Tunisia and affect the weather conditions mainly of the

southern part of the Mediterranean region. The cyclogenesis area over the Gulf of Sidra is the second but very important cyclogenesis area in NW Africa (Maheras et al. 2001), the other being the Atlas Mountain range in Algeria and Morocco. Cyclogenesis events over this region are more frequent in spring and are mainly due to thermal causes favored by the intense temperature gradient between the coast of Libya and central Sahara which is maximum during spring (Morris 1973).

CC7 (eastern Europe) includes 1682 depressions that appear throughout the year with the highest frequency during the warmer months (April–August). These depressions are formed in eastern Europe and affect the surrounding areas as well as the central and eastern regions of the northern Mediterranean basin.

CC8 (Iberia lows) is the cluster with the largest number of cyclone tracks (3181), and the associated cyclones appear throughout the year and especially during the warmer

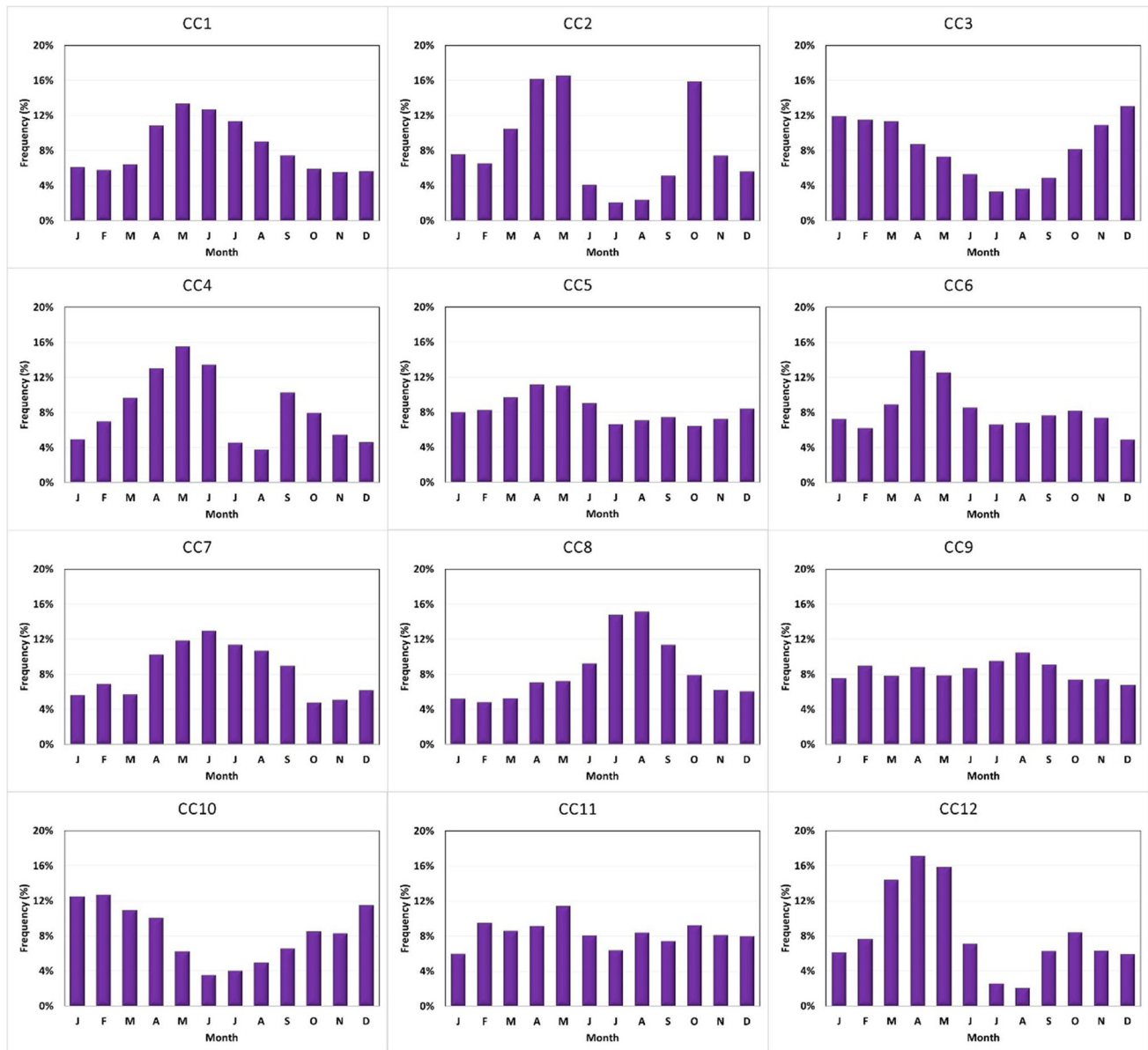


Fig. 7 The inter-monthly variations of the frequencies (%) of the 12 cyclone tracks clusters

months (July–August). Their high frequency during summer and their formation over the land of the Iberian Peninsula reveal that they are mainly of a thermal origin. The relatively warm land and sea-land contrast favor the formation of thermal lows in the Iberian Peninsula in late spring and throughout the summer (Trigo et al. 1999). These lows affect the weather of the western Mediterranean region.

CC9 (North-West Med) is the cluster with the second largest number of cyclones (3166), which appear throughout the year. The cyclogenesis areas of these depressions are mainly in the northern central Mediterranean including the Gulf of Genoa and the Alps, and affect almost the entire Mediterranean region, except its southeastern part.

The cyclogenesis in the Ligurian Sea (including the Gulf of Genoa), characterized by the well-known Alpine cyclogenesis conceptual model (Buzzi and Tibaldi 1978), is one of the main cyclogenesis cores of the entire Mediterranean region and one of the most persistent during the year (Trigo et al. 1999; Maheras et al. 2001).

CC10 (Levantine basin) comes third in the number of cyclones (2745), and the specific cyclones appear mainly during the cold period of the year (December–April). These depressions are mainly formed around the region of Cyprus and affect the weather in the areas of the eastern and central Mediterranean (Maheras et al. 2001). According to the work of Kallos and Metaxas (1980), the formation of lows

Table 1 Cyclone clusters with names, seasonality (months with frequency exceeding 10%), average central MSLP, number of cyclones classified, and mean annual frequency

CC	Name	Seasonality	Average central MSLP (hPa)	Number of cyclones	Mean annual frequency (number of cyclones per year)
1	Central Europe	April–July	1.005,6	1.546	22,4
2	Cyprus lows	March–May, October	1.008,5	833	12,1
3	North Med – cold season	November–March	1.007,1	1.617	23,4
4	Sharav cyclones – Africa	March–June, September	1.009,1	1.684	24,4
5	Black Sea	March–May, whole year	1.008,1	1.861	27,0
6	Sharav cyclones – central Med	April–May	1.008,7	1.605	23,3
7	Eastern Europe	April–August	1.005,3	1.682	24,4
8	Iberia lows	July–September	1.010,8	3.181	46,1
9	North-West Med	August, whole year	1.009,5	3.166	45,9
10	Levantine basin	December–April	1.008,6	2.745	39,8
11	East Atlantic	May, whole year	1.001,2	1.711	24,8
12	Sharav cyclones – Levantine	March–May	1.007,9	773	11,2
Total		April–May, whole year	1.007,6	22.404	324,7

in the region of Cyprus in winter is related to the invasion of cold air in the Mediterranean, being associated with the positive vorticity advection in the upper levels. Still, during the winter, there is a significant number of cyclones that form in the southeastern Aegean, consistent with the peak of the annual cyclogenesis frequency in this area (Flocas and Karacostas 1996).

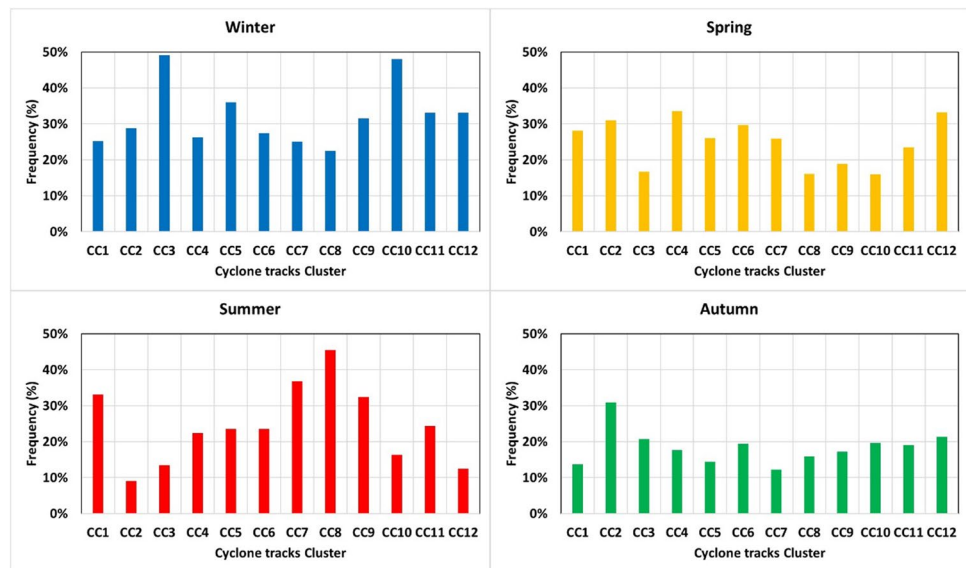
CC11 (East Atlantic) consists of 1711 cyclones which are characterized by similar frequency of occurrence in all months of the year. The depressions of this cluster mainly enter the region from the North Atlantic and/or are formed in Great Britain, and move towards the Mediterranean, affecting the weather of western Europe and western Mediterranean. The cyclonic activity over these areas may also be affected by the North Atlantic Oscillation (NAO) which is the main large-scale oscillation that significantly affects the atmospheric circulation, primarily by regulating the occurrence of the Atlantic blocking (Prezerakos 1985) and the shift of the synoptic scale atmospheric circulation from zonal to meridional over this part of the greater Mediterranean region (Hurrell and Van Loon 1997), favoring the intrusion of the cyclonic activities from northern into southern latitudes.

Finally, CC12 (Sharav cyclones, Levantine) consists of the smallest number of cyclones (773), which are most common in spring. During this season, there is a characteristic increase in the appearance of cyclones in North Africa, known as the Saharan depressions, as has also been noted in previous studies (Flocas 1988; Prezerakos et al. 1990; Trigo et al. 1999). This is the third cluster of cyclones which originate in northern Africa, the others being CC4 and CC6. However, what differentiates this cluster from the other two is that the cyclones of this

cluster mostly dominate over NE Africa and moving in a direction from SW to NE significantly affects the weather conditions in the eastern Mediterranean.

This objective clustering algorithm suggests that the classes commonly used to describe Mediterranean cyclones can be further detailed. All clusters corresponding to Sharav cyclones (CC4, CC6, CC12) have their maximum frequency in the first semester of the year with most cyclogenesis occurring south of the Atlas mountains. These three clusters differ because, as cyclogenesis areas move eastward, most cyclone tracks remain above Africa (CC4), cross the western and central Mediterranean basins (CC6), or the Levantine basin (CC12). Cyprus lows are included in both CC2 and CC10. In the latter cluster (CC10), they are the main components of a broad system that affects the whole Levantine basin initiating from the Adriatic Sea with a maximum in the coldest part of the year. In the former cluster (CC2), they correspond more to the usual connotation of Cyprus cyclones that are described as eastward moving systems that are generated south of Anatolia and occur mostly in the transitional periods of the year (CC2 shows its maximum frequencies in May and October). The northern Mediterranean Sea is confirmed to be a strong cyclogenetic area (CC3 and CC9). The two clusters differ, as CC3 represents cyclones whose frequency has a large annual cycle (with a broad maximum in the cold part of the year) and a core generation area south of the Alps, while CC9 represents cyclones occurring almost uniformly during the year, with a generation area in the northwestern Mediterranean (including the well-known cyclogenetic area of the Gulf of Genoa). The overall annual cycle (Fig. 4) hides the heterogeneity of the different clusters and does not reflect specifically that of any cluster.

Fig. 8 The frequency distributions (%) of the 12 defined cyclone clusters (CCs) for each season



3.2 Definition of the Mediterranean seasons

In the next step, PCA is applied to the smoothed (5-day moving average) mean intra-annual variations of the frequencies of which the 12 CCs and 4 PCs are retained, accounting for 83% of the total variance. CA is then applied to the time-series of the 4 PCs classifying the 365 dates of the year into four clusters based on the frequency distributions between the 12 CCs, which can be considered as the four objectively defined seasons. Figure 8 shows the frequency distributions (%) of the 12 defined CCs for each season, thus revealing the connection between the cyclone types and the seasons. Specifically, winter is characterized more by the presence of CCs 3 and 10 (North Med, cold season and Levantine basin cyclones), which, together, provide the bulk of the winter storm track crossing the Mediterranean Sea in the southeastward direction. Spring is characterized with high frequency of CCs 4, 6, and 12 (Sharav cyclones); CC1 (central Europe); and CC2 (Cyprus lows), while CCs 3 and 10 characterized winter, and CCs 8 and 9 are comparatively less frequent. In summer, CCs 1, 7, and 8 (central Europe, eastern Europe, Iberia) with a core activity over land areas are the most frequent (particularly the thermal lows of CC8, Iberia cyclones), with an important presence of CC9 (North-West Med), which, however, has no marked seasonality. Finally, autumn shows higher frequency of CC2 (Cyprus lows), while all other CCs are present with low and similar frequencies.

The limits and durations of the four seasons defined by the cyclone tracks' frequency variation (hereafter called CTF) method are shown in Fig. 9a, where the distances of the dates from the centers of the clusters (seasons) are shown. For each date, the Euclidian distance from each cluster center is calculated (shown by different colors),

and it is classified to the cluster/season from the center of which has the smallest distance. As a result, 4 seasons were defined which are similar to the conventional ones, but show significant differences in the limits and the continuity as the seasons are intertwined. Particularly, a peculiarity of the CFT classification is that autumn conditions appear to occur systematically for short periods in winter and spring. According to the CTF method, "winter" includes the period 14–25 November, 30 November–12 January, and 18 January–27 March and lasts more than 4 months (125 days); "spring" is the period 4 April–7 May and May 12–June 14 lasting a week more than 2 months (68 days); "summer" begins on June 15 and ends on September 26 with a duration of 104 days; and "autumn" includes the dates September 27–November 13, 26–29 November, 13–17 January, 28 March–3 April, and 8 May–11 May and lasts a little over 2 months (68 days).

Figure 9 also shows the seasons defined with the MVV and WTF methods applied in Kotsias et al. 2020b) and Kotsias et al. (2021).

According to the MVV method (Fig. 9b), the characteristics of the respective seasons are as follows: "winter" is the period November 24–March 20 with a duration of almost 4 months (117 days), "spring" follows until June 12 and lasts a week less than 3 months (84 days), "summer" (June 13–September 7) has a duration of about 3 months (87 days), and finally "autumn" (September 8–November 23) closes the cycle with a duration of 2.5 months (77 days).

According to the WTF method (Fig. 9c), "winter" (November 26–March 20) lasts almost 4 months (115 days), "spring" is the period March 21–May 31 with a duration of about 2.5 months (72 days), "summer" follows until September 22 with a duration of almost 4 months (114 days),

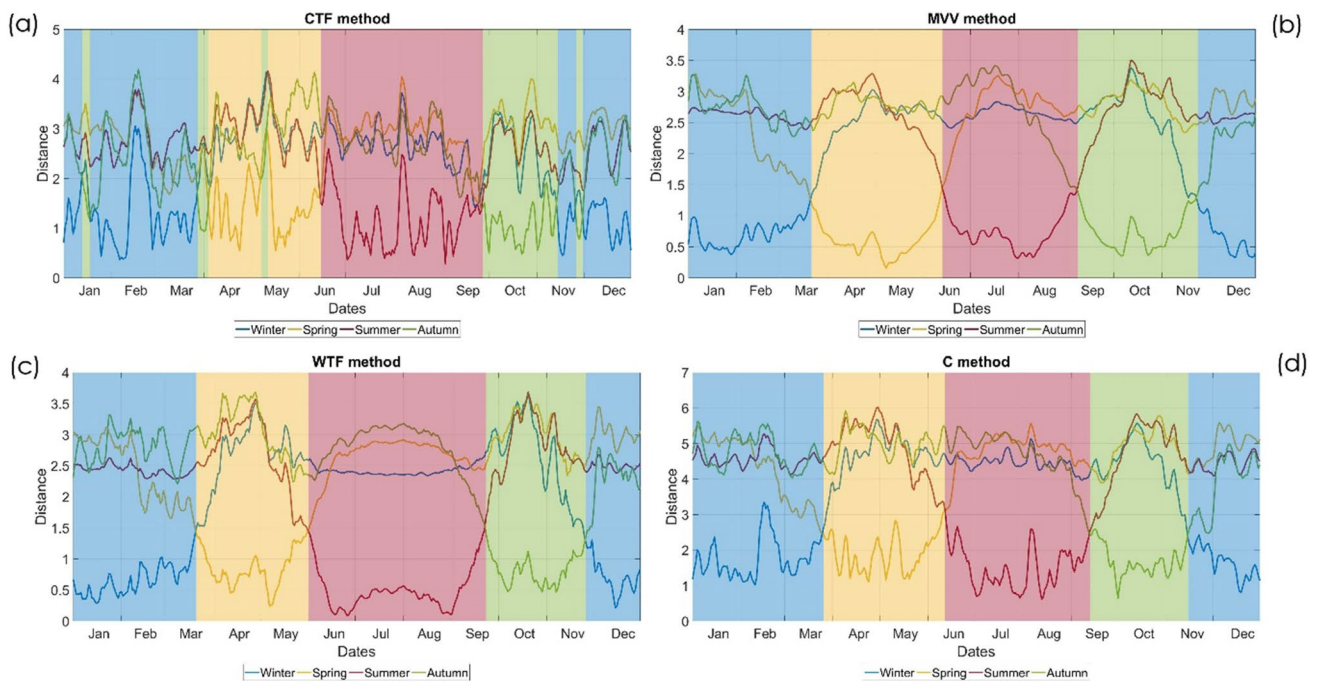


Fig. 9 The intra-annual variations of the Euclidean distances of the 4 objectively defined seasons from the centers of the clusters for the period 1949–2018 as calculated by the methods **a** CTF, **b** MVV, **c** WTF, and **d** C

Table 2 The start/end dates and durations of the four objectively defined seasons for each method (CTF, MVV, WTF, C)

Season →	Winter			Spring		
Method ↓	Start date	End date	Duration	Start date	End date	Duration
CTF method	14–25 November, 30 November–12 January, 18 January–27 March		125	4 April–7 May, 12 May–14 June		68
MVV method	24 November	20 March	117	21 March	12 June	84
WTF method	26 November	20 March	115	21 March	31 May	72
C method	16 November	25 March	131	26 March	11 June	78
Season →	Summer			Autumn		
Method ↓	Start date	End date	Duration	Start date	End date	Duration
CTF method	15 June	26 September	104	27 September–13 November, 26–29 November, 13–17 January, 28 March–3 April, 8 May–11 May		68
MVV method	13 June	7 September	87	8 September	23 November	77
WTF method	1 June	22 September	114	23 September	25 November	64
C method	12 June	12 September	93	13 September	15 November	63

and “autumn” is the period September 23–November 25 and lasts almost 2 months (64 days).

Finally, the composition (C method) of the above three approaches, i.e., the CTF method, the MVV method, and the WTF method, is applied. The results are presented in Fig. 9d and are as follows: “winter” begins on November 16 and ends on March 25 and lasts more than 4 months (131 days), “spring” follows until June 11 with a duration of approximately 2.5 months (78 days), “summer” begins on June 12 and ends on September 12 and lasts 3 months (93 days), and finally “autumn” closes the annual cycle

(September 13–November 15) with a duration of 2 months (63 days).

Table 2 shows the start and end dates as well as the duration of each season for each of the four approaches. For winter, method C has defined the longest duration, with the CTF method following, while the MVV and WTF methods have defined almost the same winter duration. The spring defined by the MVV method is longer than that of the other approaches, while the one defined by the CTF method is the shortest. Summer shows the biggest differences. In descending order, the duration of summer defined by the

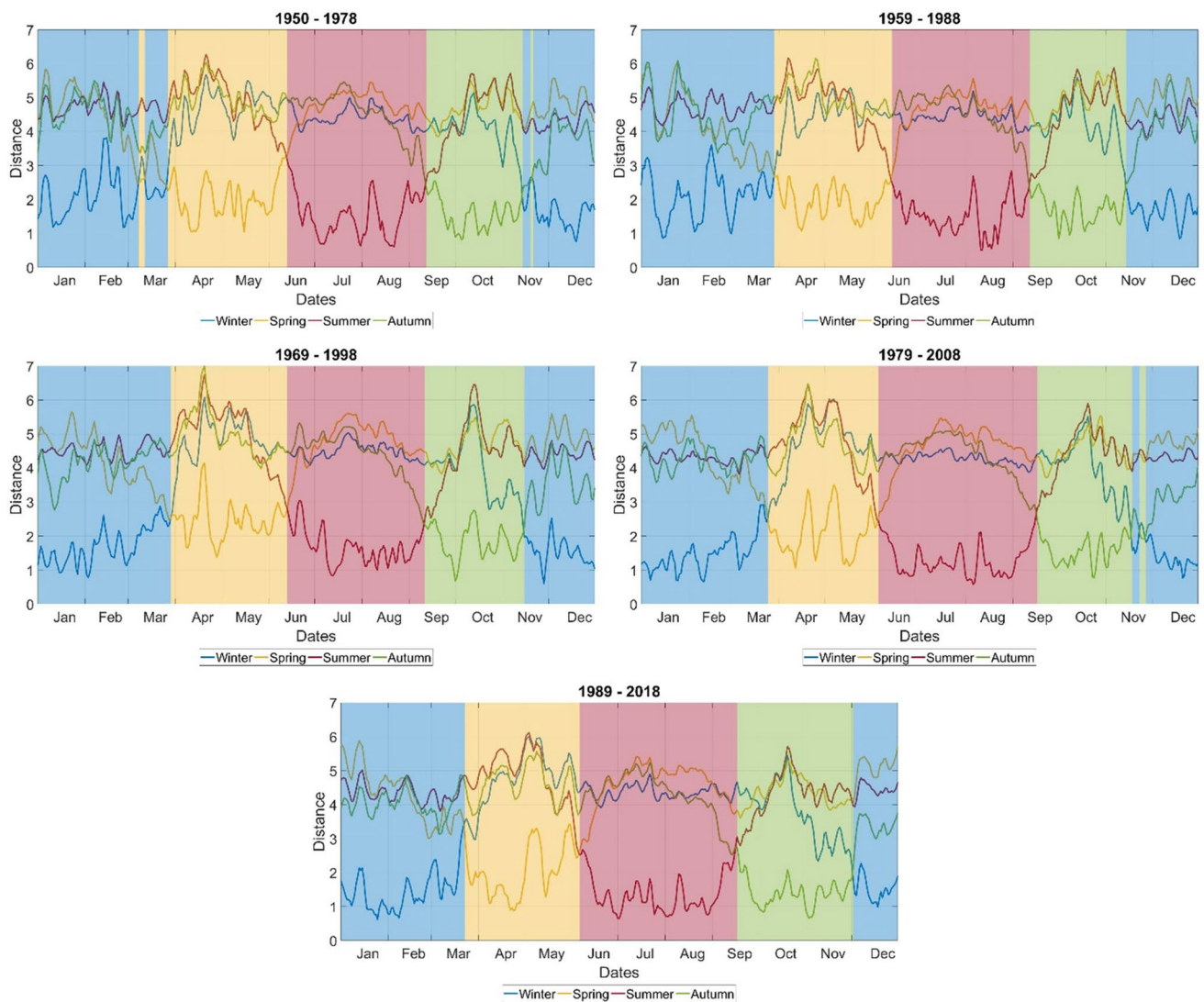


Fig. 10 The intra-annual variations of the distances of the 4 objectively defined seasons from the centers of the clusters, for the C method, for the five overlapping 30-year subperiods 1950–1978, 1959–1988, 1969–1998, 1979–2008, and 1989–2018

four methods is 114 days (WTF), 104 days (CFT), 93 days (C), and 87 days (MVV), with the difference between the WTF and MVV methods reaching almost 1 month. Finally, the autumn determined by the MVV method is the longest, while the autumn defined by the C method is the shortest.

In order to reveal any long-term changes in the characteristics of the seasons, the above four methods have been applied to all five overlapping 30-year subperiods 1950–1978, 1959–1988, 1969–1998, 1979–2008, and 1989–2018. For all five subperiods and for all methods, 4 seasons are defined. Figure 10 shows the intra-annual variations of the distances of the 4 objectively defined seasons from the centers of the clusters, for the composite method (C method), for these five subperiods. Even though 4 seasons are determined in every period, there are a few cases where a season is not contiguous and there is

a brief intermission with its adjacent seasons (e.g., 23–26 November of 1979–2008). This issue, which complicates the delimitation of the seasons, mainly derives from the smaller number of available years relatively to the full period (30 years instead of 70), which leads to less stable statistical parameters (long-term averages).

To account for this difficulty, we calculate two start and two end dates for each season. The first start dates refer to the first appearance of the seasons, while the second start dates refer to their second appearance after the short intermission by its adjacent season, when it exists. A similar calculation is carried out for the end dates of the seasons. The two start/end dates and the duration of the seasons for each 30-year subperiod are shown in Fig. 11. The duration of the seasons presented is the total number of dates classified in the corresponding cluster. The most remarkable changes of

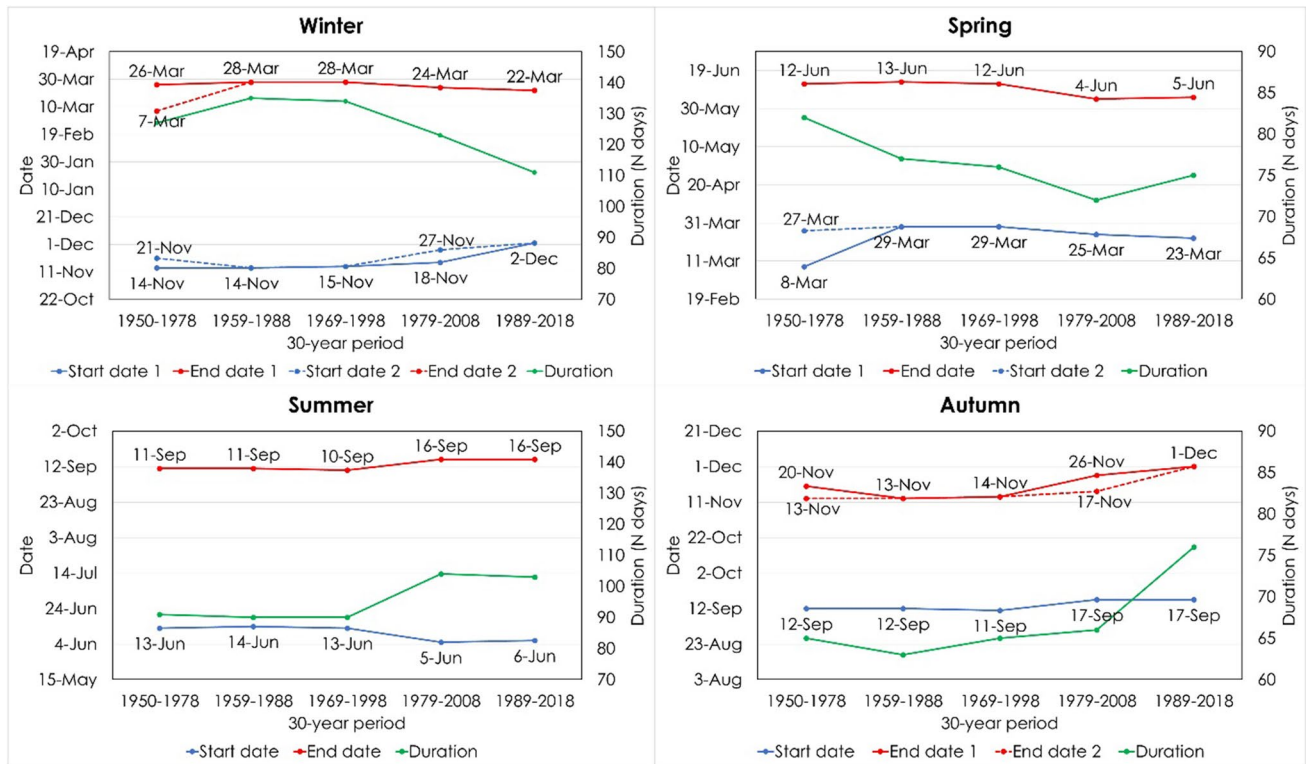


Fig. 11 The long-term variations of the start and end dates and the duration of the 4 objectively defined seasons for the composite (C) method

the seasons' characteristics are the following. The end date of winter seems to move a little earlier in every period, and winter arrives later in recent years, resulting in a shortening of the winter duration after the third subperiod. With regard to spring, the start/end dates move earlier in the last periods, and as a consequence, there is a general shortening of spring. In the two most recent subperiods, summer came earlier and ended later and as such its duration increased. Finally, in recent years, autumn comes and goes later and its duration increased.

Interesting remarks can be made by comparing the findings of the present study with those of previous works. Cheng and Kalkstein (1997) utilized the frequency of seasonal air masses to objectively define the seasons in the East Coast of the USA and found significant spatial differences of the characteristics of the seasons. Comparing their results with those of the C method, it can be said that the seasons determined here for the Mediterranean are more similar to those defined in the mid-Atlantic region of the USA, where two longer seasons (summer and winter) lasting almost 4 months each and 2 shorter seasons (spring and autumn) being approximately 2 months each were found. Alpert et al. (2004b) attempted to objectively define the limits of the seasons in the eastern Mediterranean by using the frequency of occurrence of the prevalent synoptic systems defined in Alpert et al. (2004a). Comparing their results with the ones of the C method applied

here, Alpert et al. found that winter starts later and is shorter, spring comes later and leaves earlier and thus is also shorter, summer comes earlier and ends later and thus is longer, and autumn is also longer since it ends later. It is worth noting that the seasons defined by Alpert et al. are more similar to those resulting from the application of the WTF method. Ajjur and Al-Ghamdi (2021) applied the MVV method to objectively determine the seasons in the Arabian Peninsula and found that winter (2 November–31 January) lasts 91 days, spring follows until 22 May lasting 111 days, summer extends for 106 days until 5 September, and autumn closes the annual cycle with a duration of 57 days. Comparing those seasons with those determined by the C method, as well as the MVV method applied for the Mediterranean, Ajjur and Al-Ghamdi found shorter winter and autumn seasons and longer spring and summer seasons. As expected, the meteorological parameters involved, the methodology applied, and the region of interest affect the delimitation of the seasons and lead to different results, but commonalities can also be found.

4 Conclusions

In the present work, an objective cyclone detection and tracking analysis is carried out for the Mediterranean region for the time period 1950–2018. The method (Lionello et al.

2002) uses high-resolution 6-hourly mean sea-level pressure data from the ERA5 database. “Spectral analysis” (principal component analysis followed by cluster analysis) is applied in order to classify the resulting cyclone tracks into groups/clusters, resulting into the formation of 12 cyclone tracks clusters. Successively, “spectral analysis” is applied to the time-series of the intra-annual variations of the cyclone tracks clusters’ frequencies, and four seasons are defined (cyclone tracks’ frequency (CTF) method). These seasons generally correspond to the conventional ones (winter, spring, summer, autumn) but present differences in their limits and duration. The results are also compared with the seasons defined by two other methods from previous studies: the meteorological variables’ mean intra-annual variation (MVV) method introduced in Kotsias et al. (2020b), and the weather types’ frequency (WTF) method followed by Kotsias et al. (2021). Finally, a composite (C) method is applied which combines the CTF, MVV, and WTF methods. The main conclusions that can be derived from this study are:

- 1 Approximately 325 cyclones are detected each year with the highest frequency of cyclone activity during late spring. The main cyclogenesis and high-density areas of cyclones are the Gulf of Genoa, the Atlas Mountain range, the Cyprus region, the Black Sea, and the Middle East.
- 2 “Spectral analysis”, consisting of principal component analysis (PCA) followed by cluster analysis (CA), has produced 12 clusters of cyclones, defined according to their spatial distribution including cyclogenesis areas, track characteristics, persistence throughout the year, and areas affected. The clusters with the highest number of classified cyclones are those whose cyclogenesis occurs around the Iberian Peninsula, over the Gulf of Genoa on the lee of the Alps, in N Africa, in the Cyprus region, and in the Middle East.
- 3 The application of “spectral analysis” on the intra-annual variations of the frequencies of the 12 cyclone clusters (CTF method) has led to four objectively defined seasons, which generally correspond to the conventional ones, but presented differences in their limits and duration. In short, the CTF method revealed longer winter and summer seasons and shorter spring and autumn seasons, compared to the conventional ones.
- 4 According to the composite (C) method, which combines three methods of objective definition of seasons, the seasons are: “winter” (November 16–March 25) lasts more than 4 months (131 days), “spring” (March 26–June 11) has a duration of approximately 2.5 months (78 days), “summer” (June 12–September 12) lasts 3 months (93 days), and “autumn” (September 13–November 15) closes the cycle with a duration of 2 months (63 days).
- 5 Changes of the limits and duration of the seasons have been investigated by considering the C method and five overlapping 30-year subperiods: 1950–1978, 1959–1988, 1969–1998, 1979–2008, and 1989–2018. There is a clear indication that “winter” has become progressively shorter (mostly because of its earlier onset in the recent decades) and “summer” longer (because it both starts earlier and terminates later after the mid-70 s than previously). In the last decades, the duration of “autumn” has become longer because its delayed termination prevails over its later onset. The duration of “spring” presents smaller changes with respect to other seasons, with a small shortening caused by its earlier termination.

The study of cyclones and their characteristics is a subject which has been examined in depth in atmospheric sciences. There are multiple cyclone detection and tracking algorithms that have applied throughout the years by utilizing different parameters and methodologies, but the improvements of databases with higher spatial and temporal resolutions and the increasing computing capabilities lead to new and interesting findings. On the other hand, the objective definition of the seasons and their characteristics is a subject not widely explored. Future work could include other methods for the determination of seasons, such as the use of phenology, extreme weather events, and global oscillations’ indices. Furthermore, it could be interesting to split the Mediterranean region into parts, i.e., northern–southern part, in order to investigate possible spatial differences of the seasons’ characteristics. However, it is worth noting that the present study, which combines three different methods of objective seasons’ definition (intra-annual variations of meteorological variables, frequency of weather types, and frequency of cyclone tracks), is a complete effort which provides a “new” insight and is an important addition to the scientific community of climate research.

Acknowledgements This research was supported by the project “Dioni: Computing Infrastructure for Big-Data Processing and Analysis” (MIS No. 5047222) co-funded by the European Union (ERDF) and Greece through the Operational Program “Competitiveness, Entrepreneurship and Innovation”, NSRF 2014-2020. The MSLP data are obtained from the ERA5 reanalysis dataset <https://cds.climate.copernicus.eu/cdsapp#!/home>.

Author contribution All authors contributed to the study conception and design. Material preparation, data collection, and analysis were performed by G Kotsias. The first draft of the manuscript was written by G Kotsias and CJ Lolis. All authors read and approved the final manuscript.

Funding Open access funding provided by HEAL-Link Greece. The corresponding author received funding from the project “Dioni: Computing Infrastructure for Big-Data Processing and Analysis” (MIS No. 5047222) co-funded by European Union (ERDF) and Greece through

the Operational Program “Competitiveness, Entrepreneurship and Innovation”, NSRF 2014–2020.

Data and code availability The data sets analyzed during the current study are available in the ERA5: Copernicus Climate Change Service (C3S) repository, <https://cds.climate.copernicus.eu/cdsapp#!/home>. The modified data and the code used for the plots and the diagrams are available on request. The cyclone detection and tracking algorithm was developed by Lionello P. and is also available on request (only for research, not for commercial applications).

Declarations

Ethics approval The study does not contain research involving human participants and/or animals, and it does involve the informed consent principle.

Consent to participate and consent for publication All authors consent to participate and to the publication of the study.

Competing interests The authors declare no competing interests.

Open Access This article is licensed under a Creative Commons Attribution 4.0 International License, which permits use, sharing, adaptation, distribution and reproduction in any medium or format, as long as you give appropriate credit to the original author(s) and the source, provide a link to the Creative Commons licence, and indicate if changes were made. The images or other third party material in this article are included in the article’s Creative Commons licence, unless indicated otherwise in a credit line to the material. If material is not included in the article’s Creative Commons licence and your intended use is not permitted by statutory regulation or exceeds the permitted use, you will need to obtain permission directly from the copyright holder. To view a copy of this licence, visit <http://creativecommons.org/licenses/by/4.0/>.

References

- Ajjur SB, Al-Ghamdi SG (2021) Seventy-year disruption of seasons characteristics in the Arabian Peninsula. *Int J Climatol* 41(13):5920–5937. <https://doi.org/10.1002/joc.7160>
- Akperov MG, Bardin MY, Volodin EM, Golitsyn GS, Mokhov II (2007) Probability distributions for cyclones and anticyclones from the NCEP/NCAR reanalysis data and the INM RAS climate model. *Izvestiya Atmos Ocean Phys* 43:705–712. <https://doi.org/10.1134/S0001433807060047>
- Alpert P, Osetinsky I, Ziv B, Shafir H (2004a) Semi-objective classification for daily synoptic systems: application to the Eastern Mediterranean climate change. *Int J Climatol* 24(8):1001–1011. <https://doi.org/10.1002/joc.1036>
- Alpert P, Osetinsky I, Ziv B, Shafir H (2004b) A new seasons definition based on classified daily synoptic systems: an example for the Eastern Mediterranean. *Int J Climatol* 24(8):1013–1021. <https://doi.org/10.1002/joc.1037>
- Bartholy J, Pongrácz R, Pattantyús-Ábrahám M (2009) Analyzing the genesis, intensity, and tracks of western Mediterranean cyclones. *Theor Appl Climatol* 96:133–144. <https://doi.org/10.1007/s00704-008-0082-9>
- Bartzokas A, Metaxas DA (1995) Factor Analysis of some climatological elements in Athens, 1931–1992: covariability and climatic change. *Theor Appl Climatol* 52(3–4):195–205. <https://doi.org/10.1007/BF00864043>
- Blender R, Fraedrich K, Lunkeit F (1997) Identification of cyclone-track regimes in the North Atlantic. *Q J Roy Meteor Soc* 123:727–741. <https://doi.org/10.1002/qj.49712353910>
- Buzzi A, Tibaldi S (1978) Cyclogenesis in the lee of the Alps: a case study. *Q J Roy Meteor Soc* 104:271–287. <https://doi.org/10.1002/qj.49710444004>
- Campins J, Genovés A, Picornell MA, Jansà A (2011) Climatology of Mediterranean cyclones using the ERA-40 data set. *Int J Climatol* 31(11):1596–1614. <https://doi.org/10.1002/joc.2183>
- Chambers EW, Colin de Verdière É, Erickson J, Lazard S, Lazarus F, Thite S (2009) Homotopic Fréchet distance between curves, or walking your dog in the woods in polynomial time. *Comp Geom - Theor Appl* 43(3):295–311. <https://doi.org/10.1016/j.comgeo.2009.02.008>
- Cheng S, Kalkstein LS (1997) Determination of climatological seasons for the East Coast of the U.S. using an air mass-based classification. *Clim Res* 8:107–116. <https://doi.org/10.3354/cr008107>
- Copernicus Climate Change Service (C3S) (2017) ERA5: fifth generation of ECMWF atmospheric reanalyses of the global climate. Copernicus Climate Change Service Climate Data Store (CDS), 21/11/2019. <https://cds.climate.copernicus.eu/cdsapp#!/home>
- Flaounas E, Kotroni V, Lagouvardos K, Flaounas I (2014) CycloTRACK (v1. 0) tracking winter extratropical cyclones based on relative vorticity: sensitivity to data filtering and other relevant parameters. *Geosci Model Dev* 7:1841–1853. <https://doi.org/10.5194/gmd-7-1841-2014>
- Flaounas E, Davolio S, Raveh-Rubin S, Pantillon F, Miglietta MM, Gaertner MA, Hatzaki M, Homar V, Khodayar S, Korres G, Kotroni V, Kushta J, Reale M, Ricard D (2022) Mediterranean cyclones: current knowledge and open questions on dynamics, prediction, climatology and impacts. *Weather Clim Dynam* 3:173–208. <https://doi.org/10.5194/wcd-3-173-2022>
- Flocas AA (1988) Frontal depressions over the Mediterranean Sea and central southern Europe. *Me’diterrane’e* 4:43–52
- Flocas HA, Karacostas TS (1996) Cyclogenesis over the Aegean Sea: identification and synoptic categories. *Meteorol Appl* 3:53–61. <https://doi.org/10.1002/met.5060030106>
- Hersbach H, Bell B, Berrisford P, Hirahara S, Horányi A, Muñoz-Sabater J, Nicolas J, Peubey C, Radu R, Schepers D, Simmons A, Soci C, Abdalla S, Abellan X, Balsamo G, Bechtold P, Biavati G, Bidlot J, Bonavita M, De Chiara G, Dahlgren P, Dee D, Diamantakis M, Dragani R, Flemming J, Forbes R, Fuentes M, Geer A, Haimberger L, Healy S, Hogan RJ, Hólm E, Janisková M, Keeley S, Laloyaux P, Lopez P, Lupu C, Radnoti G, de Rosnay P, Rozum I, Vamborg F, Villaume S, Thépaut JN (2020) The ERA5 global reanalysis. *Q J Roy Meteor Soc* 146(730):1999–2049. <https://doi.org/10.1002/qj.3803>
- Hoskins BJ, McIntyre ME, Robertson AW (1985) On the use and significance of isentropic potential vorticity maps. *Q J Roy Meteor Soc* 111(470):877–946. <https://doi.org/10.1002/qj.49711147002>
- Hurrell JW, Van Loon H (1997) Decadal variations in climate associated with the North Atlantic oscillation. *Clim Change* 36(3–4):301–326. <https://doi.org/10.1023/a:1005314315270>
- Inatsu M (2009) The neighbor enclosed area tracking algorithm for extratropical wintertime cyclones. *Atmos Sci Lett* 10:267–272. <https://doi.org/10.1002/asl.238>
- Jolliffe IT (1986) *Principal Component Analysis*. New York: Springer. <https://www.springer.com/gp/book/9780387954424>
- Kalkstein LS, Barthel CD, Greene JS, Nichols MC (1996) A new spatial classification: application to air-mass analysis. *Int J Climatol* 16(9):983–1004. [https://doi.org/10.1002/\(SICI\)1097-0088\(199609\)16:9%3c983::AID-OC61%3e3.0.CO;2-N](https://doi.org/10.1002/(SICI)1097-0088(199609)16:9%3c983::AID-OC61%3e3.0.CO;2-N)
- Kallos G, Metaxas A (1980) Synoptic processes for the formation of Cyprus lows. *Riuista di Meteorologia Aeronautica* XL(2–3):121–138

- Kendall M (1975) *Multivariate analysis*. Charles Griffin, London, p 210
- Kotsias G, Lolis CJ, Hatzianastassiou N, Levizzani V, Bartzokas A (2020) On the connection between large-scale atmospheric circulation and winter GPCP precipitation over the Mediterranean region for the period 1980–2017. *Atmos Res* 233:104714. <https://doi.org/10.1016/j.atmosres.2019.104714>
- Kotsias G, Lolis CJ, Hatzianastassiou N, Lionello P, Bartzokas A (2020b) An objective definition of seasons for the Mediterranean region. *Int J Climatol* 41:E1889–E1905. <https://doi.org/10.1002/joc.6819>
- Kotsias G, Lolis CJ, Hatzianastassiou N, Lionello P, Bartzokas A (2021) A comparison of different approaches for the definition of seasons in the Mediterranean region. *Int J Climatol* 42:1954–1974. <https://doi.org/10.1002/joc.7345>
- Lionello P, Dalan F, Elvini E (2002) Cyclones in the Mediterranean region: the present and the doubled CO2 climate scenarios. *Clim Res* 22:147–159. <https://doi.org/10.3354/cr022147>
- Lionello P, Bhend J, Buzzi A, Della-Marta PM, Krichak SO, Jansa A, Maheras P, Sanna A, Trigo IF, Trigo R (2006) Cyclones in the Mediterranean region: climatology and effects on the environment. *Dev Earth Environ Sci* 4:325–372. [https://doi.org/10.1016/S1571-9197\(06\)80009-1](https://doi.org/10.1016/S1571-9197(06)80009-1)
- Lionello P, Abrantes F, Congedi L, Dulac F, Gacic M, Gomis D, ..., Xoplaki E (2012) Introduction: Mediterranean climate-background information. In *The climate of the Mediterranean region: From the past to the future* (pp. xxxv–xc). Elsevier Inc., <https://doi.org/10.1016/B978-0-12-416042-2.00012-4>
- Lionello P, Trigo I, Gil V, Liberato M, Nissen K, Pinto J, Raible C, Reale M, Tanzarella A, Trigo R, Ulbrich S, Ulbrich U (2016) Objective climatology of cyclones in the Mediterranean region: a consensus view among methods with different system identification and tracking criteria. *Tellus Series A: Dyn Meteorol Ocean* 68. <https://doi.org/10.3402/tellusa.v68.29391>
- Maheras P, Flocas HA, Patrikas I, Anagnostopoulou C (2001) A 40 year objective climatology of surface cyclones in the Mediterranean Region: spatial and temporal distribution. *Int J Climatol* 21(1):109–130. <https://doi.org/10.1002/joc.599>
- Metaxas DA (1978) Evidence on the importance of diabatic heating as a divergence factor in the Mediterranean. *Archiv für Meteorologie, Geophysik Und Bioklimatologie, Series A* 27:69–80
- Morris RM (1973) *The origin structure and movement of the Saharan depressions. In brief notes on synoptic meteorology in the Mediterranean region*. Meteorological Office College: Shinfield Park, Reading, UK
- Murray RJ, Simmonds I (1991) A numerical scheme for tracking cyclone centres from digital data. Part I: development and operation of the scheme. *Australian Meteorological Magazine* 39
- Neu U, Akperov MG, Bellenbaum N, Benestad R, Blender R et al (2013) IMILAST: a community effort to intercompare extratropical cyclone detection and tracking algorithms. *B Am Meteorol Soc* 94(4):529–547. <https://doi.org/10.1175/BAMS-D-11-00154.1>
- Pinto JG, Spanghel T, Ulbrich U, Speth P (2005) Sensitivities of a cyclone detection and tracking algorithm: individual tracks and climatology. *Meteorol Z* 14:823–838. <https://doi.org/10.1127/0941-2948/2005/0068>
- Prezerakos NG (1995) The northwest african depressions affecting the south Balkans. *Int J Climatol* 5(6):643–654. <https://doi.org/10.1002/joc.3370050606>
- Prezerakos NG, Michaelides SC, Vlassi AS (1990) Atmospheric synoptic conditions associated with the initiation of north-west African depressions. *Int J Climatol* 10:711–729. <https://doi.org/10.1002/joc.3370100706>
- Raible CC, Della-Marta P, Schwierz C, Wernli H, Blender R (2008) Northern Hemisphere extratropical cyclones: a comparison of detection and tracking methods and different reanalyses. *Mon Weather Rev* 136:880–897. <https://doi.org/10.1175/2007MWR2143.1>
- Reale M, Lionello P (2013) Synoptic climatology of winter intense precipitation events along the Mediterranean coasts. *Nat Hazards Earth Sys Sci* 13:1707–1722. <https://doi.org/10.5194/nhess-13-1707-2013>
- Richman MB (1986) Rotation of Principal Components. *Int J Climatol* 6(3):293–335. <https://doi.org/10.1002/joc.3370060305>
- Shapiro MA, Keyser D (1990) Fronts, jet streams and the tropopause. In: Newton, C.W., Holopainen, E.O. (eds) *Extratropical Cyclones*. Am Meteorol Soc, Boston, MA. https://doi.org/10.1007/978-1-944970-33-8_10
- Sharma S (1995) *Applied multivariate techniques*. New York, ISBN: 978-0471310648: John Wiley & Sons, p. 512
- Simmonds I, Murray RJ (1999) Southern extratropical cyclone behavior in ECMWF analyses during the FROST special observing periods. *Weather Forecast* 14:878–891. [https://doi.org/10.1175/1520-0434\(1999\)014%3c0878:SECBIE%3e2.0.CO;2](https://doi.org/10.1175/1520-0434(1999)014%3c0878:SECBIE%3e2.0.CO;2)
- Sinclair MR (1997) Objective identification of cyclones and their circulation, intensity and climatology. *Weather Forecast* 12:591–608. <http://www.jstor.org/stable/26244647>
- Sugar CA, James GM (2003) Finding the number of clusters in a dataset. *J Am Stat Assoc* 98(463):750–763. <https://doi.org/10.1198/016214503000000666>
- Thorncroft C, Flocas H (1997) A case study of Saharan cyclogenesis. *Mon Weather Rev* 125:1147–1165. [https://doi.org/10.1175/1520-0493\(1997\)125%3c1147:ACSOSC%3e2.0.CO;2](https://doi.org/10.1175/1520-0493(1997)125%3c1147:ACSOSC%3e2.0.CO;2)
- Trigo IF (2006) Climatology of interannual variability of storm-tracks in the Euro-Atlantic sector: a comparison between ERA-40 and NCEP/NCAR reanalyses. *Clim Dynam* 26:127–143. <https://doi.org/10.1007/s00382-005-0065-9>
- Trigo IF, Davies TD, Bigg GR (1999) Objective climatology of cyclones in the Mediterranean region. *J Climate* 12(6):1685–1696. [https://doi.org/10.1175/1520-0442\(1999\)012%3c1685:OCOCIT%3e2.0.CO;2](https://doi.org/10.1175/1520-0442(1999)012%3c1685:OCOCIT%3e2.0.CO;2)
- Trigo IF, Bigg GR, Davies TD (2002) Climatology of cyclogenesis mechanisms in the Mediterranean. *Mon Weather Rev* 130:549–569. [https://doi.org/10.1175/1520-0493\(2002\)130%3C0549:COC-MIT%3E2.0.CO;2](https://doi.org/10.1175/1520-0493(2002)130%3C0549:COC-MIT%3E2.0.CO;2)
- Wang XL, Swail VR, Zwiers FW (2006) Climatology and changes of extra-tropical cyclone activity: comparison of ERA-40 with NCEP/NCAR reanalysis for 19582001. *J Climate* 19:3145–3166. <https://doi.org/10.1175/JCLI3781.1>
- Wernli H, Schwierz C (2006) Surface cyclones in the ERA-40 data set (1958–2001). Part I: novel identification method and global climatology. *J Atmos Sci* 63:2486–2507. <https://doi.org/10.1175/JAS3766.1>

Publisher's note Springer Nature remains neutral with regard to jurisdictional claims in published maps and institutional affiliations.